2

Correlations, nonlocality, and usefulness of an efficient class of two-qubit mixed entangled states

2.1 INTRODUCTION

The use of entangled resources for efficient communication in comparison to their classical counterparts is based on the existence of long-range correlations between entangled qubits [Bennett and Wiesner, 1992; Bennett *et al.*, 1993; Zukowski *et al.*, 1993; Boström and Felbinger, 2002; Gisin *et al.*, 2002]. Such correlations not only distinguish between the quantum and classical world, but also provide a deeper physical interpretation to fundamentals of quantum theory and applications of information processing [Einstein *et al.*, 1935; Bohm and Aharonov, 1957; Batle *et al.*, 2002; Batle and Casas, 2011; Batle *et al.*, 2016, 2017]. In general, for a bipartite system, the distinction between quantum and classical resources is laid down in terms of Bell-type inequalities whose violation confirms the existence of quantum correlations in the system [Bell, 1964; Clauser *et al.*, 1969]. Bell-type inequalities, however, do not account for all nonclassical properties of entangled qubits in mixed states. For example, one can find a mixed bipartite state which may be entangled but would still not violate the Bell-type inequality [Werner, 1989; Horodecki, 1996; Ma *et al.*, 2015]. The characterization and usefulness of such systems for quantum communication and information processing would certainly help us to have a better insight into the nature of quantum correlations. Moreover, recent studies in quantum information have shown that the relationship between nonclassicality and correlations is not limited to entangled systems only, but can also be extended to some separable systems [Knill and Laflamme, 1998; Luo, 2008a; Datta *et al.*, 2008; Dakić *et al.*, 2010; Zhang *et al.*, 2012]. The degradation of entanglement and quantum correlation under real experimental set-ups leads to further questions regarding usefulness of final resources due to interactions with the environment [Zurek, 2003; Almeida *et al.*, 2007]. In general, the finally shared state will always be a mixed state. Hence, besides the fundamental quest to understand the nature of quantum correlations, it is also important to analyse and characterize the nonlocal properties of finally shared mixed state so that one can take informed decisions as to whether it is useful or not to use the finally shared state for quantum information processing. Fortunately, entanglement can be protected against noise by performing weak measurements [Korotkov and Keane, 2010; Lee *et al.*, 2011; Kim *et al.*, 2012]. The role of correlations in quantum information and communication is, therefore, still requires a much deeper analysis to understand the significance of quantum correlations in security, communication and information processing.

In this chapter, therefore, we revisit the question of analysing the usefulness of quantum correlations under noisy conditions and weak measurements. For this, we derive an analytical relation between the Bell-CHSH inequality, state parameter, noise parameters and strength of weak measurements. Our results show some interesting observations regarding applications of weak measurement and its reversal operations under amplitude-damping, phase-damping, and depolarizing noise. In case of amplitude-damping channels, the analysis further allows us to propose a class of two-qubit mixed entangled states which does not violate the Bell inequality for weak measurement strength less than $\frac{1}{2}$ but is still useful in quantum information processing. Our analysis shows that these states, although not violating the Bell inequality, are still entangled and have non-zero discord [Luo, 2008a; Dakić *et al.*, 2010]. We further investigate the usefulness of such a class for quantum information processing in terms of teleportation fidelity [Horodecki *et al.*,

1996, 1999a], witness operators [Horodecki, 1996; Terhal, 2000], and channel capacity for dense coding protocol [Bowen, 2001]. The analysis shows that our states can indeed be used for successful information processing protocols for certain ranges of noise and weak measurement strength. Interestingly, we found that the states proposed here can be characterized as efficient and useful resources for quantum information processing protocols in comparison to a large set of randomly sampled bipartite mixed and pure states. However, in case of phase-damping channels, we found that the extent of violation of the Bell-CHSH inequality is independent of the state parameter and weak measurement strength for optimal weak measurement reversal strength, hence, bringing in the flexibility to start with any initial state instead of starting with a maximally entangled states only. On the other hand, if we fix the value of reverse weak measurement, then the expectation value of Bell-CHSH operator first increases, attains a maximum value and then decreases again. For depolarizing noise as well, we found that the weak measurements may be useful for protecting nonlocal correlations against the noise.

2.2 NONLOCALITY, NOISE AND WEAK MEASUREMENTS

The violation of Bell-CHSH inequality revealed the fundamentally different nature of quantum theory in comparison to local hidden variable theories. In the generalized case, if Alice and Bob choose their measurements as A or A' and B or B' with equal probability of $\frac{1}{2}$ then the Bell-CHSH inequality can be represented as

$$\left|E\left(AB\right)+E\left(AB'\right)+E\left(A'B\right)-E\left(A'B'\right)\right|\leq 2 \tag{2.1}$$

such that $A=\sigma_1.\hat{a}$, and $A'=\sigma_1.\hat{a}'$, where $\hat{a}$, $\hat{a}'$ are unit vectors and σ_i's are spin projection operators. The measurement operators B and B' can be defined in a similar fashion. In general, states violating the Bell-CHSH inequality are considered to be useful resources in quantum information and computation. However, presence of noise hinders the efficiency of such systems due to degradation of correlations between the qubits. In order to protect entanglement and quantum correlations from decoherence, several models such as entanglement distillation [Bennett *et al.*, 1996b,a; Pan *et al.*, 2003b], decoherence free subspace [Lidar *et al.*, 1998; Kwiat *et al.*, 2000], quantum error correcting codes [Shor, 1995; Calderbank and Shor, 1996; Steane, 1996; Knill and Laflamme, 1997], and quantum zeno effect [Facchi *et al.*, 2004; Maniscalco *et al.*, 2008] have been proposed and studied. Recently, a new scheme is developed to protect entanglement from decoherence known as weak measurements and its reversal [Korotkov and Jordan, 2006; Kim *et al.*, 2009; Sun *et al.*, 2009; Korotkov and Keane, 2010; Cheong and Lee, 2012; Xiao and Li, 2013; Zong *et al.*, 2014; Zhang *et al.*, 2015; He and Ye, 2015; Xiao *et al.*, 2016; Huang *et al.*, 2017; Huang and Situ, 2017]. The concept of weak measurement is fundamental to quantum mechanics and is defined in terms of partial collapse measurement operators associated with positive operator valued measure. The process of weak measurement and its reversal has been found to be very useful to propose interaction free measurements [Paraoanu, 2006], and to suppress decoherence in single and two-qubit systems [Korotkov and Jordan, 2006; Bellomo *et al.*, 2008; Katz *et al.*, 2008; Kim *et al.*, 2009; Sun *et al.*, 2009; Korotkov and Keane, 2010; Barreiro *et al.*, 2010; Sun *et al.*, 2010; Paraoanu, 2011; Franco *et al.*, 2012; Cheong and Lee, 2012; Xiao and Li, 2013; Zong *et al.*, 2014; Zhang *et al.*, 2015; He and Ye, 2015; Ji and Liu, 2016; Huang and Situ, 2017]. Moreover, weak measurements have been experimentally implemented in many quantum systems [Katz *et al.*, 2006; Korotkov and Jordan, 2006; Kim *et al.*, 2009; Lee *et al.*, 2011; Kim *et al.*, 2012; Xu *et al.*, 2013; Groen *et al.*, 2013; Lim *et al.*, 2014; White *et al.*, 2016; Zou *et al.*, 2017].

The fundamental theory behind the working principle of weak measurement and its reversal operations lies in the factual possibility of reversing any partial collapse measurement. The basic approach is to perform weak measurement operations on the individual qubits comprising the quantum system before distributing entanglement through noisy channels so that the initial

state suffers less from the applied noise. After weak measurement, and entanglement distribution through decoherence channels, one performs non-unitary reversal weak measurement operations on the individual qubits to recover the quantum correlations. The optimal strength of weak measurement reversal operation, corresponding to the initial strength of weak measurement operation, can be obtained by maximizing the entanglement and correlations between the qubits. In the following sub-sections, we analyse the effect of different noise channels and weak measurements on the correlations existing between qubits of a bipartite state.

2.2.1 Amplitude-Damping Channel

We first proceed to analyse the effect of decoherence and weak measurements by establishing a relation between the maximum expectation value of the Bell-CHSH operator, state parameter, noise parameters and weak measurement strengths. For this, we start with a scenario where Charlie prepares a two-qubit pure state $|\Psi\rangle = \alpha|00\rangle + \beta|11\rangle$ $(|\alpha|^2 + |\beta|^2 = 1)$ and sends one qubit each to Alice and Bob through an amplitude-damping channel. The single-qubit Kraus operators for an amplitude-damping channel can be given as

$$E_0^i = \begin{pmatrix} 1 & 0 \\ 0 & \sqrt{1-\gamma_i} \end{pmatrix}, \quad E_1^i = \begin{pmatrix} 0 & \sqrt{\gamma_i} \\ 0 & 0 \end{pmatrix} \tag{2.2}$$

where γ represents the magnitude of decoherence, and $i = 1$ or $i = 2$, represents the qubit index. Therefore, the two-qubit pure state after passing through the amplitude-damping channel evolves as

$$\begin{aligned} \rho_A^\gamma &= \sum_{k,l\in(0,1)} \left(E_k^1 \otimes E_l^2\right) \rho \left(E_k^{\dagger 1} \otimes E_l^{\dagger 2}\right) \\ &= \begin{pmatrix} |\alpha|^2 + \gamma_1\gamma_2|\beta|^2 & 0 & 0 & \sqrt{\gamma_1'\gamma_2'}\alpha^*\beta \\ 0 & \gamma_1\gamma_2'|\beta|^2 & 0 & 0 \\ 0 & 0 & \gamma_2\gamma_1'|\beta|^2 & 0 \\ \sqrt{\gamma_1'\gamma_2'}\alpha\beta^* & 0 & 0 & \gamma_1'\gamma_2|\beta|^2 \end{pmatrix} \end{aligned} \tag{2.3}$$

where $\gamma_i' = 1 - \gamma_i$. In order to find whether the above state violates the Bell-CHSH inequality or not, we need to evaluate the maximum expectation value of the Bell-CHSH operator given in Eq. (2.1). In terms of spin projection operators, Eq. (2.1) can be re-expressed as

$$B\left(\rho_A^\gamma\right) = \left\langle \sigma_1 \cdot \hat{a}\, \sigma_2 \cdot \hat{b} \right\rangle + \left\langle \sigma_1 \cdot \hat{a}\, \sigma_2 \cdot \hat{b}' \right\rangle + \left\langle \sigma_1 \cdot \hat{a}'\, \sigma_2 \cdot \hat{b} \right\rangle - \left\langle \sigma_1 \cdot \hat{a}'\, \sigma_2 \cdot \hat{b}' \right\rangle \tag{2.4}$$

Considering a pair of mutually orthogonal unit vectors $\hat{c}, \hat{c}'$ such that $\hat{b} + \hat{b}' = 2\cos\theta\hat{c}$, and $\hat{b} - \hat{b}' = 2\sin\theta\hat{c}'$, Eq. (2.4) can be rewritten as

$$B\left(\rho_A^\gamma\right) = 2\left[\langle \sigma_1 \cdot \hat{a}\, \sigma_2 \cdot \hat{c}\rangle \cos\theta + \left\langle \sigma_1 \cdot \hat{a}'\, \sigma_2 \cdot \hat{c}' \right\rangle \sin\theta\right] \tag{2.5}$$

where unit vectors $\hat{a}$ and $\hat{c}$ are defined as

$$\begin{aligned} \hat{a} &= (\sin\theta_a\cos\phi_a, \sin\theta_a\sin\phi_a, \cos\theta_a) \\ \hat{c} &= (\sin\theta_c\cos\phi_c, \sin\theta_c\sin\phi_c, \cos\theta_c) \end{aligned} \tag{2.6}$$

Similar definitions stand for $\hat{a}'$ and $\hat{c}'$ with primes on angles. The first term, in Eq. (2.5), representing the expectation value $\langle AC\rangle$ gives

$$\begin{aligned} &\langle \sigma_1 \cdot \hat{a}\, \sigma_2 \cdot \hat{c}\rangle = \\ &\quad \left(\alpha^2 + (2\gamma_1 - 1)(2\gamma_2 - 1)\beta^2\right)\cos\theta_a\cos\theta_c + 2\alpha\beta\sqrt{1-\gamma_1}\sqrt{1-\gamma_2}\sin\theta_a\sin\theta_c\cos\phi_{ac} \end{aligned} \tag{2.7}$$

The expectation value of $\langle AC \rangle$ can be maximized with respect to θ_a, such that

$$[\langle \sigma_1 \cdot \hat{a}\, \sigma_2 \cdot \hat{c} \rangle]_{max} = [\left(\alpha^2 + (2\gamma_1 - 1)(2\gamma_2 - 1)\beta^2\right)^2 \cos^2\theta_c + 4\alpha^2\beta^2(1-\gamma_1)(1-\gamma_2)\sin^2\theta_c]^{\frac{1}{2}} \quad (2.8)$$

where we have used the fact that maximum value of $p\sin\theta_1 + q\cos\theta_1$ is $\sqrt{p^2+q^2}$ and $\cos^2\phi_{ac} = \cos^2(\phi_a + \phi_c) = 1$. Similarly, the second term representing expectation value $\langle A'C' \rangle$ gives

$$\left[\left\langle \sigma_1 \cdot \hat{a}'\, \sigma_2 \cdot \hat{c}' \right\rangle\right]_{max} = [\left(\alpha^2 + (2\gamma_1 - 1)(2\gamma_2 - 1)\beta^2\right)^2 \cos^2\theta_{c'} + 4\alpha^2\beta^2(1-\gamma_1)(1-\gamma_2)\sin^2\theta_{c'}]^{\frac{1}{2}} \quad (2.9)$$

Eq. (2.5) is maximized with respect to θ, and therefore, we have

$$\begin{aligned} B(\rho_A^{\gamma})_{max} &= 2[\left(\alpha^2 + (2\gamma_1 - 1)(2\gamma_2 - 1)\beta^2\right)^2 (\cos^2\theta_c + \cos^2\theta_{c'}) \\ &+ 4\alpha^2\beta^2(1-\gamma_1)(1-\gamma_2)(\sin^2\theta_c + \sin^2\theta_{c'})]^{\frac{1}{2}} \end{aligned} \quad (2.10)$$

To optimize the expectation value for the operator $B(\rho_A^{\gamma})$, we use the orthogonality relation between $\hat{c}$ and $\hat{c}'$ such as $\cos^2\theta_c = \sin^2\theta_{c'}$, and hence

$$B(\rho_A^{\gamma})_{opt} = 2[\left(\alpha^2 + (2\gamma_1 - 1)(2\gamma_2 - 1)\beta^2\right)^2 + 4\alpha^2\beta^2(1-\gamma_1)(1-\gamma_2)]^{\frac{1}{2}} \quad (2.11)$$

If Charlie sends both the qubits through perfect channels such that $\gamma_i = 0$, then optimized expectation value of the Bell-CHSH operator will be $2[1 + 4\alpha^2\beta^2]^{\frac{1}{2}}$ as it should be for transmission through an ideal quantum channel [Popescu and Rohrlich, 1992].

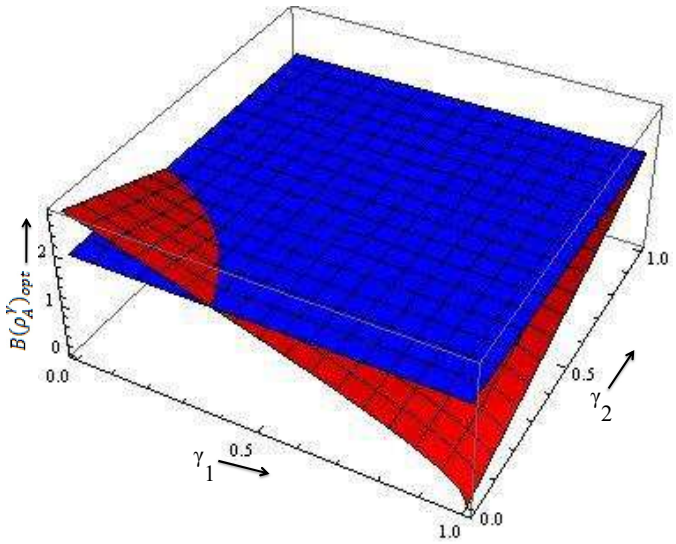

Figure 2.1 : Estimation of $B(\rho_A^{\gamma})_{opt}$ with respect to decoherence parameters γ_1 and γ_2 for a maximally entangled two-qubit state.

Figure 2.1 clearly demonstrates that the Bell-CHSH inequality is violated for a small region only where the values of noise parameters γ_i are very small; even for the violation region where the values of noise parameters are small, the violation decreases very fast. The analytical result obtained here is in complete agreement with the numerical optimization of the Bell-CHSH operator

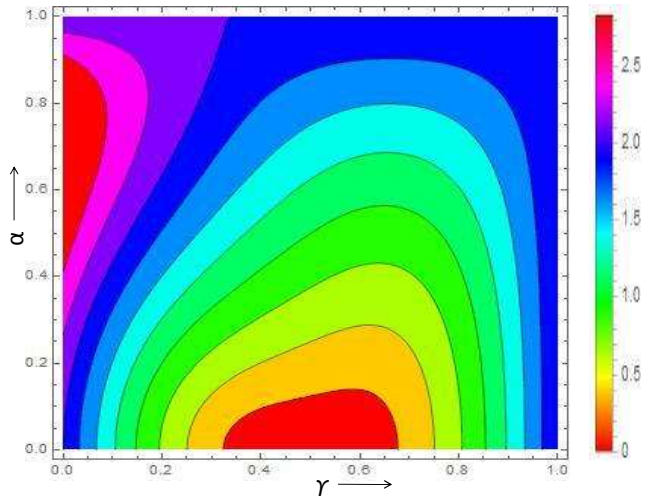

Figure 2.2 : Effect of noise parameter γ, considering (γ_1=γ_2=γ), on $B(\rho_A^\gamma)_{opt}$ for different two-qubit entangled states.

for ρ_A^γ. The effect of noise on nonlocality is also depicted in Figure 2.2 which describes the degradation of nonlocal correlations due to decoherence for different initial states, i.e., for different α values. If we consider the noise parameters to be the same then the Bell-CHSH inequality is violated by finally shared states iff $(\alpha^2+\beta^2(1-2\gamma)^2)^2+4\alpha^2\beta^2(\gamma-1)^2>1$. For example, if we start with a maximally entangled initial state, i.e., if $\alpha=1/\sqrt{2}$, then the range of decoherence parameter for the Bell inequality violation is $0\leq\gamma<0.2334$. Therefore, if we start with a maximally entangled state then finally shared state does not violate the Bell inequality for $0.2334\leq\gamma\leq1$. Interestingly, the non-violation region for a state with $\alpha=0.95$ is $0.3203\leq\gamma\leq1$, i.e., a partially entangled two-qubit state is more robust towards decoherence in comparison to a maximally entangled two-qubit state.

We now move forward to analyse the effect of weak measurements on the existence of nonlocal correlations in noisy conditions. For this, we assume that Charlie prepares a two-qubit entangled state $|\Psi\rangle=\alpha|00\rangle+\beta|11\rangle$, ($|\alpha|^2+|\beta|^2=1$), and performs weak measurements on both qubits before sending them through amplitude-damping channels. Similarly, after receiving the qubits both Alice and Bob carry out reversal of weak measurement on their qubits. The weak measurement Λ_i^{wk} and reverse weak measurement Λ_i^{wkr} operators performed at both ends can be given by

$$\Lambda_i^{wk}=\begin{pmatrix}1&0\\0&\sqrt{1-\eta_i}\end{pmatrix}\quad\Lambda_i^{wkr}=\begin{pmatrix}\sqrt{1-\eta_{ri}}&0\\0&1\end{pmatrix} \tag{2.12}$$

where η_i and η_{ri} are strengths of weak measurement and weak measurement reversal operations, respectively. The optimal weak measurement reversal strength is defined by $\eta_{ri}=\eta_i+\gamma_i(1-\eta_i)$, where $i=1,2$ [Korotkov and Keane, 2010; Lee *et al.*, 2011; Kim *et al.*, 2012]. Assuming that the strength of weak measurement reversal is optimal, the finally shared state between Alice and Bob evolves as

$$\rho_A^{wk}=\frac{1}{N_A}\begin{pmatrix}|\alpha|^2+\gamma_1\gamma_2\eta_1'\eta_2'|\beta|^2&0&0&\alpha^*\beta\\0&\gamma_1\eta_1'|\beta|^2&0&0\\0&0&\gamma_2\eta_2'|\beta|^2&0\\\alpha\beta^*&0&0&|\beta|^2\end{pmatrix} \tag{2.13}$$

where $N_A = 1 + \{\gamma_1 \eta_1'(1+\gamma_2\eta_2') + \gamma_2\eta_2'\}|\beta|^2$ and $\eta_i' = (1-\eta_i)$ and i=1,2. For analytical optimization of the Bell-CHSH operator, we first consider the first term representing expectation value $\langle AC \rangle$ in Eq. (2.5), such that

$$\begin{aligned} \langle \sigma_1 \cdot \hat{a}\, \sigma_2 \cdot \hat{c} \rangle &= \frac{1}{N_A}\left[\left(\alpha^2 + (1+\gamma_1(\eta_1-1))(1+\gamma_2(\eta_2-1))\beta^2\right)\cos\theta_a \cos\theta_c \right. \\ &+ \left. 2\alpha\beta \sin\theta_a \sin\theta_c \cos(\phi_a + \phi_c)\right] \end{aligned} \tag{2.14}$$

Similar to the way we evaluated the optimum value of Bell-CHSH operator for ρ_A^{γ}, one can show that the optimum expectation value of the Bell-CHSH operator for ρ_A^{wk} is

$$B\left(\rho_A^{wk}\right)_{opt} = \frac{2}{N_A}\left[\left(\alpha^2 + (1+\gamma_1(\eta_1-1))(1+\gamma_2(\eta_2-1))\beta^2\right)^2 + 4\alpha^2\beta^2\right]^{\frac{1}{2}} \tag{2.15}$$

For $\eta_i = 1$, the expression in Eq. (2.15) will be the same as for a pure state. This is possible since the state ρ_A^{wk} becomes a pure state, free from any decoherence for $\eta_i = 1$. Figure 2.3 demonstrates the

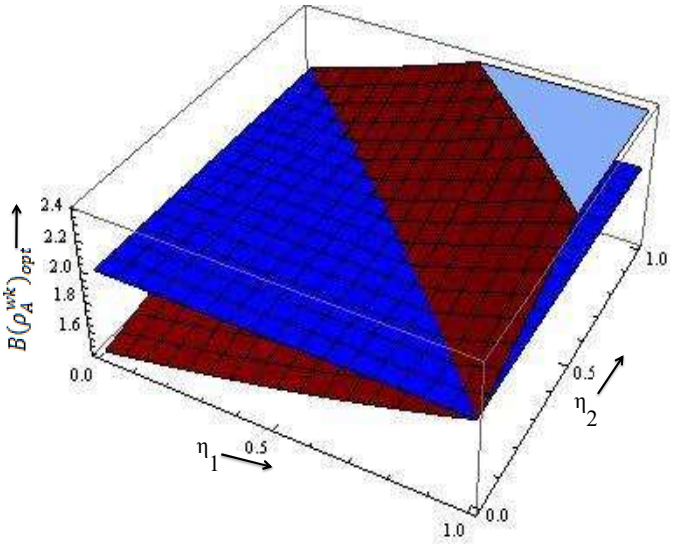

Figure 2.3 : Estimation of $B(\rho_A^{wk})_{opt}$ with respect to weak measurement strengths η_1 and η_2 for a maximally entangled initial state, considering $\gamma = 0.5$.

effect of weak measurement strengths on the Bell-CHSH operator for a decoherence parameter value of $\gamma_1 = \gamma_2 = 0.5$, and $\alpha = \frac{1}{\sqrt{2}}$. The state clearly violates the Bell-inequality for $\gamma_i = 0.5$ when the values of η_i's exceed a certain minimum, and the amount of violation increases with the increase in weak measurement strength. From Figure 2.2, one can conclude that if one starts with a maximally entangled two-qubit state then for $\gamma_i = 0.5$, the Bell-CHSH inequality is not violated. However, performing weak measurement and weak measurement reversal operations result in the violation of Bell-CHSH inequality confirming the existence of nonlocal correlations in the finally shared entangled state. For simplicity, we consider a scenario where both channels have same decoherence, i.e., $\gamma_1 = \gamma_2 = \gamma$ and both qubits are subjected to identical weak measurement strengths, i.e., $\eta_1 = \eta_2 = \eta$. In such a case, the optimal expectation value of the Bell-CHSH operator is

$$B(\rho_A^{new})_{opt} = \frac{2}{N_A'}\left[\left(\alpha^2 + (1+\gamma(\eta-1))^2\beta^2\right)^2 + 4\alpha^2\beta^2\right]^{\frac{1}{2}} \tag{2.16}$$

where $N_A' = \left(\alpha^2 + (1+\gamma(1-\eta))^2\beta^2\right)$. In order to compare the effects of weak measurement vs amplitude-damping, in Figure 2.4, we show plots between optimal expectation value of the Bell-CHSH operator and weak measurement strength for different initial states considering $\gamma = 0.6$. We consider a higher value of noise parameter as in the absence of weak measurement, the Bell-CHSH inequality is not violated by all the states. We again observe that a partially entangled

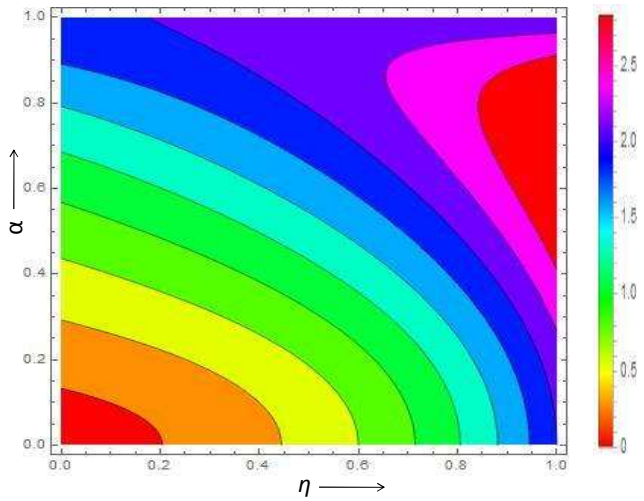

Figure 2.4 : Effect of weak measurement strength η on $B(\rho_A^{new})_{opt}$, for different two-qubit entangled states, considering the noise parameter $\gamma = 0.6$.

initial state with higher α is a better and robust resource in comparison to a maximally entangled initial state. Moreover, depending on a initial state used, the Bell-CHSH inequality is violated by the finally shared state only after a certain value of weak measurement strength η. In general the non-violation regime increases with decrease in the value of α. For a given initial state, we further deduce a condition, $\left(\left(\alpha^2 + (1+\gamma(\eta-1))^2\beta^2\right)^2 + 4\alpha^2\beta^2\right) \geq \left(\alpha^2 + (1+\gamma(1-\eta))^2\beta^2\right)^2$, for the violation of Bell-CHSH inequality by a finally shared state. For example, if $\gamma = 0.6$ then for a initial state with $\alpha = \frac{1}{\sqrt{2}}$, the strength of weak measurement required for the violation of Bell-CHSH inequality is $0.5953 \leq \eta \leq 1$.

For a maximally entangled initial state, Figure 2.5 and Figure 2.6 describe the effects of noise parameter γ for different values of weak measurement strength η and effects of weak measurement strength η for different values of noise parameter γ on maximum expectation value of the Bell-CHSH operator. Clearly weak measurement and its reversal is a win-win situation for enhancing the correlations between the qubits. Similarly, Figure 2.7 and Figure 2.8 illustrate relations between the violation of Bell-CHSH inequality and value of α for different values of noise parameter γ for $\eta = 0$, and different values of weak measurement strength for $\gamma = 0.6$, respectively.

2.2.2 Alternate method to estimate violation of the Bell-CHSH inequality

Horodecki *et al.* [Horodecki, 1995] have shown a necessary and sufficient condition for the violation of Bell-CHSH inequality by an arbitrary spin-$\frac{1}{2}$ state. According to Horodecki's theorem, maximum violation of the CHSH inequality for any arbitrary two-qubit state ρ is given by

$$B_{max}(\rho) = 2\sqrt{M(\rho)} \tag{2.17}$$

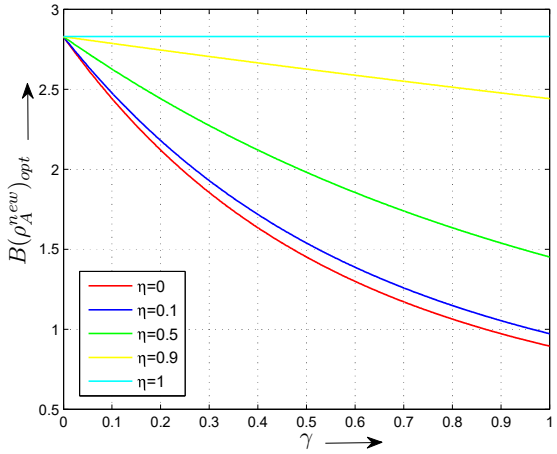

Figure 2.5 : Effect of decoherence on $B(\rho_A^{new})_{opt}$ for a maximally entangled input state at different values of weak measurement strength η.

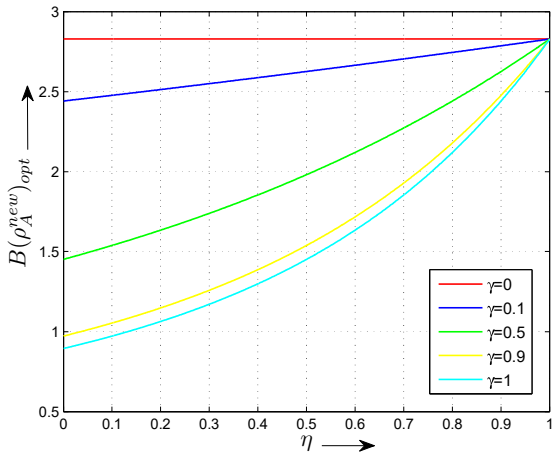

Figure 2.6 : Comparison of the Bell inequality violation vs weak measurement strength η for a maximally entangled input state at different values of decoherence parameter.

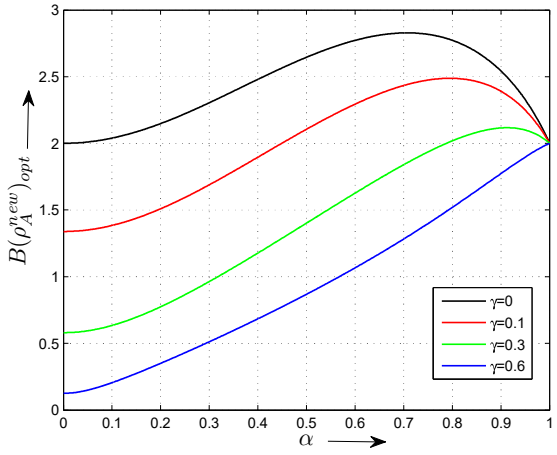

Figure 2.7 : Comparison of $B(\rho_A^{new})_{opt}$ vs state parameter α at different values of noise parameter γ, considering $\eta = 0$.

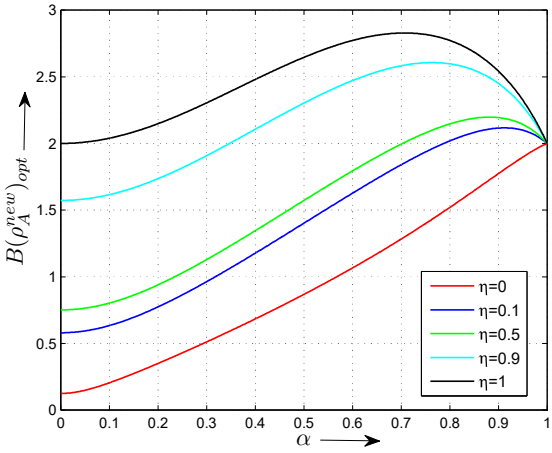

Figure 2.8 : Comparison of $B(\rho_A^{new})_{opt}$ vs state parameter α for different values of weak measurement strength, considering $\gamma = 0.6$.

where $M(\rho) = max_{i<j}(u_i + u_j)$, and $u_i (i = 1,2,3)$ are the eigenvalues of $U = T_\rho^\dagger T_\rho$. Here, $T_\rho^\dagger$ denotes the conjugate transpose of T_ρ, where T_ρ is a correlation matrix, and the inequality (2.1) is violated by an arbitrary two-qubit state iff $M(\rho) > 1$. Therefore, we calculate $M(\rho_A^{wk})$ considering identical noise parameters $\gamma_1 = \gamma_2 = \gamma$ and identical weak measurement strengths $\eta_1 = \eta_2 = \eta$, such that

$$M(\rho_A^{new}) = \frac{\left(\alpha^2 + (1+\gamma(\eta-1))^2\beta^2\right)^2 + 4\alpha^2\beta^2}{\left(\alpha^2 + (1+\gamma(1-\eta))^2\beta^2\right)^2} \tag{2.18}$$

and hence,

$$B(\rho_A^{new})_{opt} = \frac{2[\left(\alpha^2 + (1+\gamma(\eta-1))^2\beta^2\right)^2 + 4\alpha^2\beta^2]^{\frac{1}{2}}}{(\alpha^2 + (1+\gamma(1-\eta))^2)\beta^2)} \tag{2.19}$$

One can clearly see that Eq. (2.19) is the same as Eq. (2.16) obtained analytically, earlier in this chapter.

2.2.3 Phase-Damping Channel

In case of a phase-damping channel, the Kraus operators can be represented as

$$E_0 = \begin{pmatrix} 1 & 0 \\ 0 & \sqrt{1-\gamma_i} \end{pmatrix}, \quad E_1 = \begin{pmatrix} 0 & 0 \\ 0 & \sqrt{\gamma_i} \end{pmatrix} \tag{2.20}$$

where γ represents phase-damping noise parameter, and $i = 1,2$ represents the qubit index. Again, for simplicity we consider that both qubits comprising the initial input state are transmitted through identical decoherence channels, i.e., $\gamma_1 = \gamma_2 = \gamma$. Similar to the case of amplitude-damping channel, the input state shared between Alice and Bob now evolves as

$$\rho_P^\gamma = \begin{pmatrix} |\alpha|^2 & 0 & 0 & (1-\gamma)\alpha^*\beta \\ 0 & 0 & 0 & 0 \\ 0 & 0 & 0 & 0 \\ (1-\gamma)\alpha\beta^* & 0 & 0 & |\beta|^2 \end{pmatrix} \tag{2.21}$$

Therefore, using the Horodecki's theorem, optimum expectation value of the Bell-CHSH operator is given as

$$B(\rho_P^\gamma)_{opt} = 2\sqrt{1 + 4\alpha^2\beta^2(\gamma-1)^2} \tag{2.22}$$

Figure 2.9 describes the effect of decoherence on the correlations after both the qubits pass through phase-damping channels. Unlike the case of amplitude-damping channel where a non-maximally entangled state seems to be more robust than a maximally entangled state for a particular range of decoherence parameter, here the maximally entangled state is always robust in comparison to non-maximally entangled states. For a given two-qubit initial state, the finally shared state always

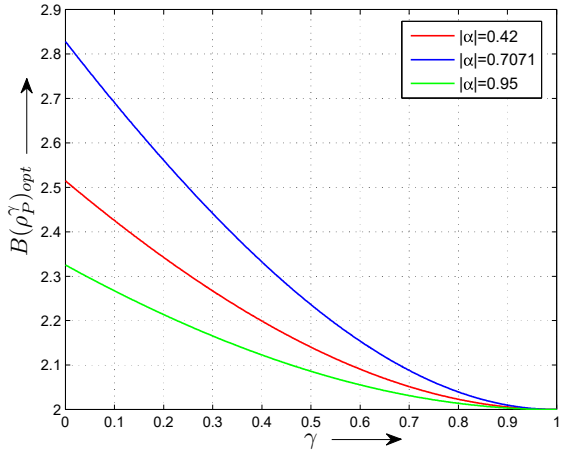

Figure 2.9 : Effect of decoherence γ on $B(\rho_P^\gamma)_{opt}$ for different two-qubit entangled states.

violates the Bell inequality for the whole range of decoherence parameter.

In order to analyse the effect of weak measurement and its reversal, we again assume that before sending the qubits through phase-damping channels, Charlie first performs weak measurements on both the qubits as given in Eq. (2.12). After receiving the qubits, Alice and Bob perform weak measurement reversal operations on their respective qubits. Therefore, the finally shared state between Alice and Bob evolves as

$$\rho_P^{wk} = \frac{1}{N_P}\begin{pmatrix} |\alpha|^2\eta_r'^2 & 0 & 0 & \alpha^*\beta\gamma'\eta'\eta_r' \\ 0 & 0 & 0 & 0 \\ 0 & 0 & 0 & 0 \\ \alpha\beta^*\gamma'\eta'\eta_r' & 0 & 0 & |\beta|^2\eta'^2 \end{pmatrix} \tag{2.23}$$

where $\eta' = (1-\eta)$, $\eta_r' = (1-\eta_r)$, $\gamma' = (1-\gamma)$, and $N_P = \left(|\alpha|^2(1-\eta_r)^2 + |\beta|^2(1-\eta)^2\right)$. The optimized value of Bell-CHSH operator for the state ρ_P^{wk} can be calculated in a similar fashion as in the case of ρ_P^γ , and can be given as

$$B\left(\rho_P^{wk}\right)_{opt} = 2\sqrt{1 + \frac{4\alpha^2\beta^2(1-\gamma)^2(1-\eta)^2(1-\eta_r)^2}{(\alpha^2(1-\eta_r)^2 + \beta^2(1-\eta)^2)^2}} \tag{2.24}$$

The optimal weak measurement reversal strength leading to maximum correlations between the qubits is evaluated to be $\eta_r = 1-(1-\eta)\frac{\beta}{\alpha}$. Hence, assuming the strength of weak measurement reversal operation to be optimal, the expectation value of Bell-CHSH operator is given as

$$B(\rho_P^{wk})_{opt} = 2\sqrt{1+(\gamma-1)^2} \tag{2.25}$$

Interestingly, Eq. (2.25) shows that the maximum expectation value of Bell-CHSH operator of a shared bipartite state is independent of the parameter α and weak measurement strength η.

Moreover, $B(\rho_P^{wk})_{opt} \geq B(\rho_P^{\gamma})_{opt}$ provided $\alpha^2\beta^2 \leq \frac{1}{2}$, which is always true for a two-qubit entangled state. Hence, the application of weak measurement can indeed be useful in upgrading the nonlocal correlations against the phase-damping decoherence. For optimal reversing weak measurement

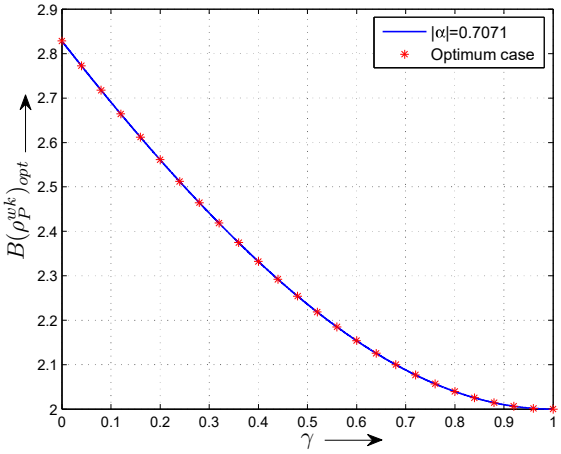

Figure 2.10 : Effect of decoherence on $B(\rho_P^{wk})_{opt}$ for a maximally entangled, and any partially entangled input state under the application of weak measurement.

strength, Figure 2.10 clearly indicates that the maximum expectation value of Bell-CHSH operator for the finally shared state does not depend on the initial input state and is always the same, as for a maximally entangled initial state. The use of weak measurement and its reversal protocol, therefore, provides a flexibility to communication protocols such that one can choose to start with any initial two-qubit pure state. However, for non-optimal weak measurement reversal, i.e.,

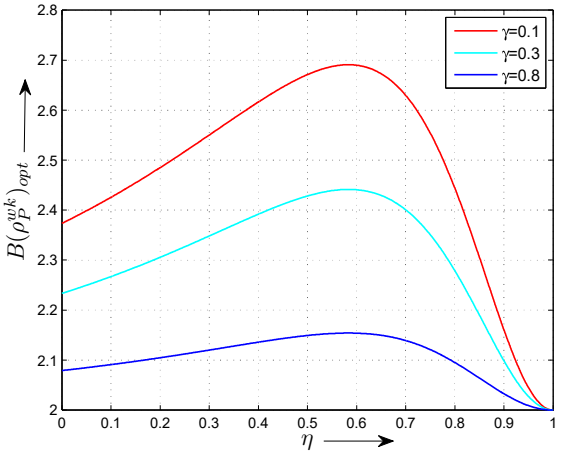

Figure 2.11 : Effect of weak measurement on $B(\rho_P^{wk})_{opt}$ for non-optimal strength of weak measurement reversal operation for different values of decoherence parameter γ, considering $\alpha = 0.42$ and $\eta_r = 0.2$.

assuming $\eta_r = 0.2$ and a given input state considering $\alpha = 0.42$, the effect of weak measurement strengths on the maximum expectation value of Bell-CHSH operator for different values of noise parameter is depicted in Figure 2.11.

2.2.4 Depolarizing Channel

Finally, we consider another important decoherence channel characterized by depolarizing noise such that the single-qubit Kraus operators are described as

$$D_0 = \sqrt{1-\gamma}\begin{pmatrix} 1 & 0 \\ 0 & 1 \end{pmatrix}, \quad D_1 = \sqrt{\frac{\gamma}{3}}\begin{pmatrix} 0 & 1 \\ 1 & 0 \end{pmatrix}$$
$$D_2 = \sqrt{\frac{\gamma}{3}}\begin{pmatrix} 1 & 0 \\ 0 & -1 \end{pmatrix}, \quad D_3 = \sqrt{\frac{\gamma}{3}}\begin{pmatrix} 0 & -i \\ i & 0 \end{pmatrix} \tag{2.26}$$

where γ is a decoherence parameter. Here, we again consider identical decoherence channels, i.e., $\gamma_1 = \gamma_2 = \gamma$. In this case, the initial state after passing through depolarizing channels can be given as

$$\rho_D^{\gamma} = \begin{pmatrix} f_{11} & 0 & 0 & f_{14} \\ 0 & f_{22} & 0 & 0 \\ 0 & 0 & f_{33} & 0 \\ f_{14}^* & 0 & 0 & f_{44} \end{pmatrix} \tag{2.27}$$

where

$$f_{11} = \frac{1}{9}\left(|\alpha|^2(3-2\gamma)^2 + 4|\beta|^2\gamma^2\right) \tag{2.28a}$$
$$f_{14} = \frac{1}{9}\alpha^*\beta(3-4\gamma)^2 \tag{2.28b}$$
$$f_{22} = f_{33} = \frac{2}{3}\gamma - \frac{4}{9}\gamma^2 \tag{2.28c}$$
$$f_{44} = \frac{1}{9}\left(|\beta|^2(3-2\gamma)^2 + 4|\alpha|^2\gamma^2\right) \tag{2.28d}$$

Thus, the optimum expectation value of $B(\rho_D^{\gamma})$ of the two-qubit state ρ_D^{γ} shared between Alice and Bob is

$$B(\rho_D^{\gamma})_{opt} = \frac{2}{9}\sqrt{(1+4\alpha^2\beta^2)(3-4\gamma)^4} \tag{2.29}$$

Figure 2.12 demonstrates the effect of noise parameter γ on the expectation value of Bell-CHSH

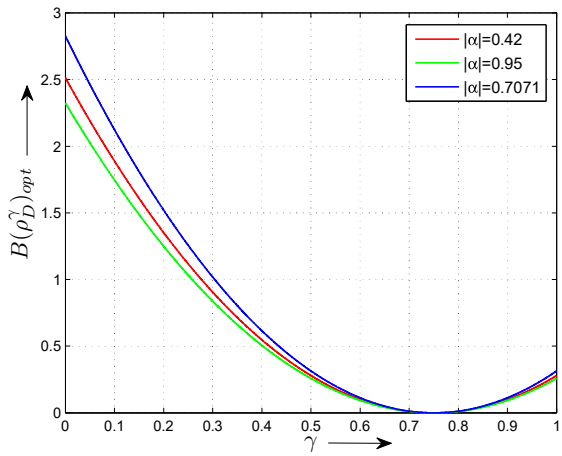

Figure 2.12 : Effect of decoherence γ on $B(\rho_D^{\gamma})_{opt}$ for different two-qubit entangled states.

operator for three different initial states, i.e., for $\alpha = \frac{1}{\sqrt{2}}$, $\alpha = 0.95$ and $\alpha = 0.42$. One can observe that the violation of Bell-CHSH inequality decreases very fast even for small values of noise parameters.

We now analyse the effect of weak measurement and quantum measurement reversal operations on nonlocal correlations of the finally shared state. For the depolarizing channel, we replace $\sqrt{1-\eta}$ with μ and $\sqrt{1-\eta_r}$ with μ_r in Eq. (2.12) such that the expressions of weak measurement and weak measurement reversal operations are now given as $\Delta^{wk} = \begin{pmatrix} 1 & 0 \\ 0 & \mu \end{pmatrix}$ and $\Delta^{wkr} = \begin{pmatrix} \mu_r & 0 \\ 0 & 1 \end{pmatrix}$, respectively [He and Ye, 2015]. Similar to the previous cases, the finally shared state between Alice and Bob evolves as

$$\rho_D^{\gamma} = \frac{1}{N_D} \begin{pmatrix} g_{11} & 0 & 0 & g_{14} \\ 0 & g_{22} & 0 & 0 \\ 0 & 0 & g_{33} & 0 \\ g_{14}^* & 0 & 0 & g_{44} \end{pmatrix} \tag{2.30}$$

where

$$N_D = g_{11} + g_{22} + g_{33} + g_{44} \tag{2.31a}$$
$$g_{11} = \mu_r^4(|\alpha|^2(3-2\gamma)^2 + 4|\beta|^2\gamma^2\mu^4) \tag{2.31b}$$
$$g_{14} = \alpha^*\beta(3-4\gamma)^2\mu^2\mu_r^2 \tag{2.31c}$$
$$g_{22} = g_{33} = 2\gamma(3-2\gamma)\mu_r^2(|\alpha|^2 + |\beta|^2\mu^4) \tag{2.31d}$$
$$g_{44} = 4|\alpha|^2\gamma^2 + |\beta|^2(3-2\gamma)^2\mu^4 \tag{2.31e}$$

The optimized value of Bell-CHSH operator for the state ρ_D^{wk} can be obtained in a similar fashion as discussed above, and can be given as

$$B\left(\rho_D^{wk}\right)_{opt} = \frac{4}{N_D}\left[2\alpha^2\beta^2(3-4\gamma)^4\mu^4\mu_r^4\right]^{\frac{1}{2}} \tag{2.32}$$

The optimal reversing weak measurement strength, in case of a depolarizing channel, for maximizing the amount of entanglement in the finally shared state is evaluated as

$$\mu_r = \left[\frac{(4|\alpha|^2\gamma^2 + |\beta|^2(3-2\gamma)^2\mu^4)}{(|\alpha|^2(3-2\gamma)^2 + 4|\beta|^2\gamma^2\mu^4)}\right]^{\frac{1}{4}} \tag{2.33}$$

Using Eq. (2.33), maximum expectation value of the Bell-CHSH operator can be achieved for $\mu^2 = |\alpha|/|\beta|$, and can be expressed as

$$B\left(\rho_D^{wk}\right)_{opt} = \frac{2}{9}\sqrt{2(3-4\gamma)^4} \tag{2.34}$$

From Eq. (2.29) and Eq. (2.34), one can further deduce that $B\left(\rho_D^{wk}\right)_{opt}$ is always greater than $B\left(\rho_D^{\gamma}\right)_{opt}$. Furthermore, for optimal weak measurement reversal strength and a maximally entangled initial input state, Figure 2.13 describes the effect of weak measurement strength on the maximum expectation value of Bell-CHSH operator considering $\gamma = 0.1$.

2.3 A NEW CLASS OF MIXED ENTANGLED TWO-QUBIT STATES

Assuming that the input state is a two-qubit pure state, the finally shared state between Alice and Bob will either be a pure or a mixed state depending on the value of weak measurement

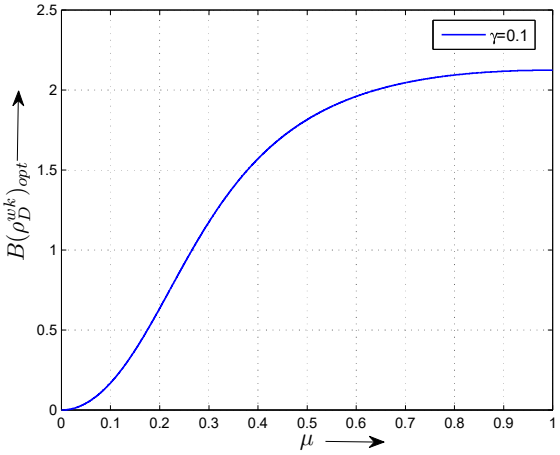

Figure 2.13 : Effect of weak measurement on $B(\rho_D^{wk})_{opt}$ for a maximally entangled initial input state, considering $\gamma = 0.1$.

strength. Recently, Y. S. Kim *et al.* [Kim *et al.*, 2012] have shown that using weak measurements in presence of amplitude-damping channels, the concurrence of the finally shared state is always non-zero, i.e., the finally shared state is always entangled. WenCho Ma *et al.* [Ma *et al.*, 2015] have extended this study and proposed a set of states which are entangled but do not violate the Bell-CHSH inequality after passing through the amplitude-damping channel. In this section, we characterize a new class of two-qubit mixed states using weak measurements under the amplitude-damping noise. Interestingly, we found that the set of states proposed here are always entangled but do not violate the the Bell-CHSH inequality for certain ranges of amplitude-damping coefficient γ and weak measurement strength η. Further, our analysis shows that these states surprisingly outperform some of the mixed states already used as resources for quantum information processing.

For this purpose, we propose a class of two-qubit mixed states as

$$\varrho = \frac{1}{N}\left[\frac{1}{2}\gamma(1-\eta)\left\{\gamma(1-\eta)\left|00\right\rangle\left\langle 00\right| + \left|01\right\rangle\left\langle 01\right| + \left|10\right\rangle\left\langle 10\right|\right\} + \left|\phi^+\right\rangle\left\langle\phi^+\right|\right] \tag{2.35}$$

where $\left|\phi^+\right\rangle = \frac{1}{\sqrt{2}}\left[\left|00\right\rangle + \left|11\right\rangle\right]$ and $N = \frac{1}{2}(2+\gamma(1-\eta)(2+\gamma(1-\eta)))$. In order to characterize the entanglement and correlations in this class, we use three different measures, i.e., Bell inequality, concurrence, and geometric discord [Bell, 1964; Wootters, 1998; Dakić *et al.*, 2010; Luo and Fu, 2010]. For example, the concurrence (in Eq. (1.7)) of the proposed class is

$$C(\varrho) = max\left\{0, \left(\frac{2-\gamma(1-\eta)}{2+\gamma(1-\eta)\left(2+\gamma(1-\eta)\right)}\right)\right\} \tag{2.36}$$

Moreover, the geometric discord for an arbitrary spin-$\frac{1}{2}$ state is represented in Eq. (1.30). Here, we are only interested in the numerical estimation of geometric discord. As discussed above, the optimal expectation value of Bell-CHSH operator for the proposed class is

$$B(\varrho) = \frac{2\left[\left(1+(1+\gamma(\eta-1))^2\right)^2+4\right]^{\frac{1}{2}}}{(1+(1+\gamma(1-\eta))^2)} \tag{2.37}$$

Figure 2.14, Figure 2.15 and Figure 2.16 demonstrate the effect of weak measurement strength η on concurrence, geometric discord, and Bell-CHSH inequality for $\gamma = 0.6$, respectively. It is

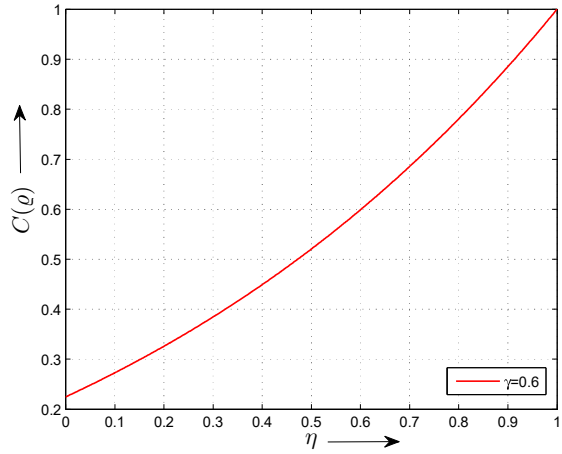

Figure 2.14 : Concurrence of the proposed state ϱ as a function of weak measurement strength, considering $\gamma = 0.6$.

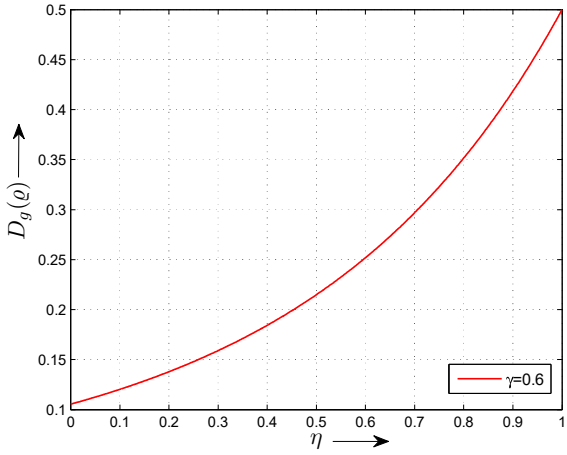

Figure 2.15 : Geometric discord of the proposed state ϱ as a function of weak measurement strength, considering $\gamma = 0.6$.

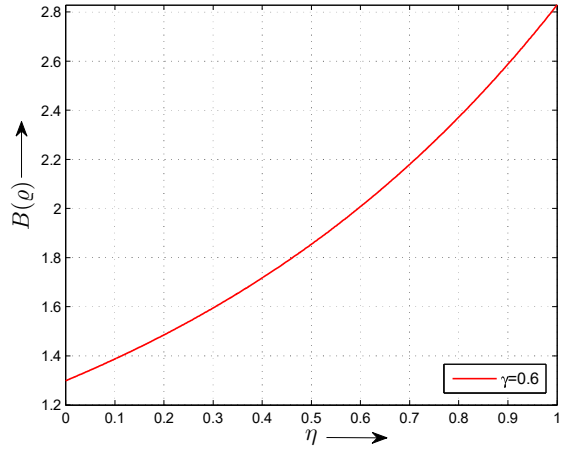

Figure 2.16 : The optimal expectation value of Bell-CHSH operator of the proposed state ϱ as a function of weak measurement strength, considering $\gamma = 0.6$.

evident that the proposed class (ϱ) shows genuine entanglement and quantum correlations for all η but violates the Bell-CHSH inequality for a range of weak measurement strength, i.e., for $max\left\{0,\left(1-\frac{0.2428}{\gamma}\right)\right\}<\eta\leq 1$.

2.4 USEFULNESS OF THE PROPOSED TWO-QUBIT MIXED STATES IN INFORMATION PROCESSING TASKS

In this section, we demonstrate the efficiency and usefulness of proposed class of states in terms of quantum teleportation, dense coding, and fully entangled fraction.

2.4.1 Quantum Teleportation

Quantum teleportation allows a sender to communicate quantum information using an entangled resource without sending the information through any medium. Horodecki *et al.* [Horodecki *et al.*, 1996] described a measure of usefulness for two-qubit mixed entangled states in terms of fidelity of quantum teleportation, namely

$$F_{max}(\rho)=\frac{1}{2}\left[1+\frac{H(\rho)}{3}\right] \tag{2.38}$$

where $H(\rho)=\Sigma_{i=1}^{3}\sqrt{u_i}$ and $u_i(i=1,2,3)$ are the eigenvalues of a real symmetric matrix $U_\rho=T_\rho^T T_\rho$. They further deduced that a given state is useful as a resource for quantum teleportation iff $H(\rho)>1$. In this sub-section, we show that the class of states proposed in the previous section can always be used as a resource for quantum teleportation irrespective of the strength of decoherence and weak measurements. Surprisingly, when it comes to the fidelity of quantum teleportation, our states outperform many other mixed entangled two-qubit states. For this, we first calculate $H(\varrho)$ for the proposed state ϱ, such that

$$H(\varrho)=4\sqrt{\frac{1}{(1+(1+\gamma(1-\eta))^2)^2}}+\sqrt{\frac{(1+(1+\gamma(\eta-1))^2)^2}{(1+(1+\gamma(1-\eta))^2)^2}} \tag{2.39}$$

and hence,

$$F_{max}(\varrho)=\frac{1}{2}\left[1+\frac{4}{3}\sqrt{\frac{1}{(1+(1+\gamma(1-\eta))^2)^2}}+\frac{1}{3}\sqrt{\frac{(1+(1+\gamma(\eta-1))^2)^2}{(1+(1+\gamma(1-\eta))^2)^2}}\right] \tag{2.40}$$

Figure 2.17 clearly indicates that teleportation fidelity using our states is always greater than $2/3$. Therefore, states of the proposed class are useful resources for quantum teleportation irrespective of the values of noise parameter for the whole range of weak measurement parameter η.

Further, we compare the efficiency of our states as resources for teleportation fidelity with other existing bipartite mixed states. We first consider the two-qubit mixed Werner state [Werner, 1989], i.e.,

$$\rho_w=(1-x)\frac{I_4}{4}+x\left|\psi^+\right\rangle\left\langle\psi^+\right| \tag{2.41}$$

where x stands for probability, I stands for identity matrix representing a white noise and $|\psi^+\rangle$ represents a maximally entangled Bell state, given by

$$\left|\psi^+\right\rangle=\frac{1}{\sqrt{2}}\left[|01\rangle+|10\rangle\right] \tag{2.42}$$

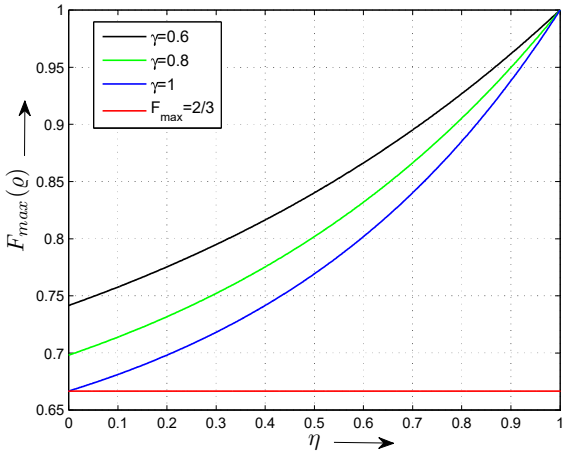

Figure 2.17 : Teleportation fidelity of the proposed state ϱ as a function of weak measurement strength η at different values of decoherence parameter γ.

The teleportation fidelity of Werner states using Eq. (2.38) is

$$F_{max}(\rho_w) = \frac{(x+1)}{2} \tag{2.43}$$

Similarly, for Horodecki states [Horodecki, 1996], namely

$$\rho_h = (1-a)\left|00\right\rangle\left\langle 00\right| + a\left|\psi^+\right\rangle\left\langle\psi^+\right| \tag{2.44}$$

where a stands for the state parameter, teleportation fidelity can be evaluated as

$$F_{max}(\rho_h) = \begin{cases} \frac{2}{3} & a \leq \frac{1}{2} \\ \frac{(2a+1)}{3} & a > \frac{1}{2} \end{cases} \tag{2.45}$$

We further consider another important class of two-qubit mixed states [Munro *et al.*, 2001b], termed as maximally entangled mixed states (MEMS), given by

$$\rho_{MEMS} = \begin{pmatrix} z(\delta) & 0 & 0 & \frac{\delta}{2} \\ 0 & 1-2z(\delta) & 0 & 0 \\ 0 & 0 & 0 & 0 \\ \frac{\delta}{2} & 0 & 0 & z(\delta) \end{pmatrix} \tag{2.46}$$

where

$$z(\delta) = \begin{cases} \frac{1}{3} & \delta < \frac{2}{3} \\ \frac{\delta}{2} & \delta \geq \frac{2}{3} \end{cases} \tag{2.47}$$

with δ, a state parameter, denoting the concurrence of ρ_{MEMS}. One can calculate the optimal teleportation fidelity for ρ_{MEMS}, such that

$$F_{max}(\rho_{MEMS}) = \begin{cases} \frac{(3\delta+5)}{9} & \delta < \frac{2}{3} \\ \frac{(2\delta+1)}{3} & \delta \geq \frac{2}{3} \end{cases} \tag{2.48}$$

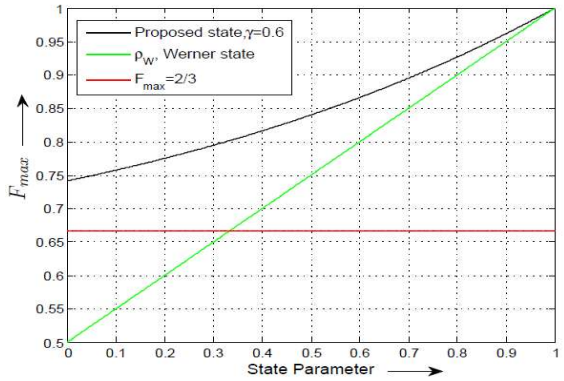

2.18 (a) : Comparison of the teleportation fidelity of proposed class of states and Werner state.

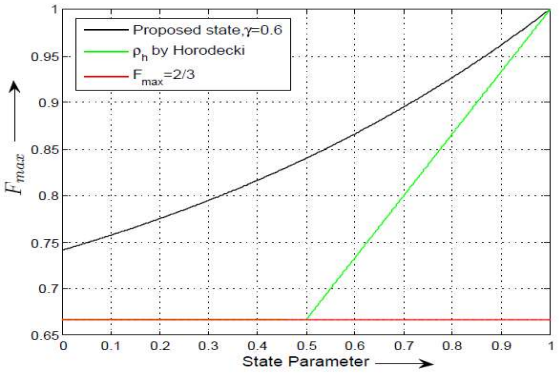

2.18 (b) : Comparison of the teleportation fidelity of proposed class of states and Horodecki state.

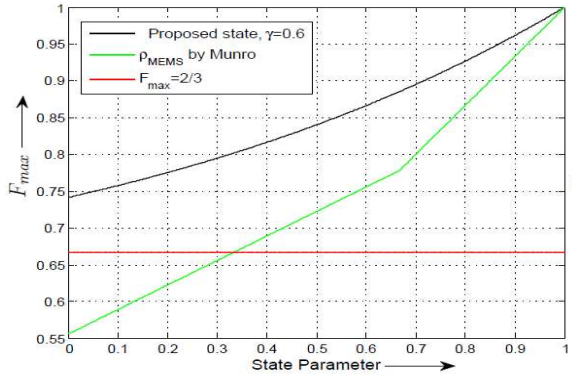

2.18 (c) : Comparison of the teleportation fidelity of proposed class of states and MEMS state proposed by Munro *et. al.*

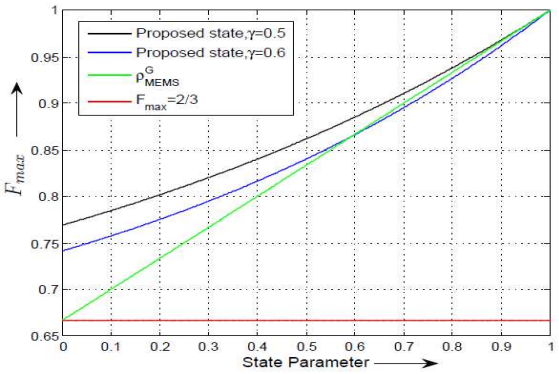

2.18 (d) : Comparison of the teleportation fidelity of proposed class of states and generalized MEMS state proposed by Wei *et. al.*

Figure 2.18 : Comparison of usefulness of the proposed state with other existing bipartite entangled mixed states.

A more general class of maximally entangled mixed states was proposed by Wei *et al.* [Wei *et al.*, 2003] as a mixture of a maximally entangled Bell state $|\phi^+\rangle$ and a mixed diagonal state. Therefore, the general form of MEMS is given by

$$\rho^G_{MEMS} = \begin{pmatrix} q+\frac{\lambda}{2} & 0 & 0 & \frac{\lambda}{2} \\ 0 & s & 0 & 0 \\ 0 & 0 & t & 0 \\ \frac{\lambda}{2} & 0 & 0 & r+\frac{\lambda}{2} \end{pmatrix} \tag{2.49}$$

where q, r, s, t, and λ are non-negative real state parameters such that $(q+r+\lambda+s+t) = 1$. The teleportation fidelity for ρ^G_{MEMS} is given by

$$F_{max}(\rho^G_{MEMS}) = \frac{2}{3} + \frac{1}{3}(\lambda - s - t) \tag{2.50}$$

From Eq. (2.50), the optimal teleportation fidelity of ρ^G_{MEMS} can be obtained by considering $s = 0, t = 0$ such that we get

$$F_{max}(\rho^G_{MEMS}) = \frac{2}{3} + \frac{\lambda}{3} \tag{2.51}$$

Figure 2.18 compares the efficiency of the proposed state in this chapter with the two-qubit Werner, Horodecki, ρ_{MEMS}, and ρ^G_{MEMS} states for quantum teleportation. It clearly shows that the states

proposed here can always be considered as better resources in comparison to Werner states, Horodecki states, and ρ_{MEMS} states. In case of ρ^{G}_{MEMS} states, our states prove to be better resources for teleportation under weak decoherence, however, for strong decoherence either our states or ρ^{G}_{MEMS} states can be considered as preferred resources depending on the values of state parameters. Moreover, for $s \neq 0$ or $t \neq 0$, the proposed states will always be better resources for teleportation as compared to ρ^{G}_{MEMS} states.

2.4.2 Fully-Entangled Fraction

Our analysis in the last subsection suggests that the proposed state is always a better resource in comparison to other established two-qubit mixed states for quantum teleportation protocol. In this subsection, we extend our analysis to fully-entangled fraction (FEF) f_{ent} which is an entanglement witness, and can be defined as

$$f_{ent}(\rho) = \max_{\phi} \langle \phi | \rho | \phi \rangle \tag{2.52}$$

where the maximum is taken over all maximally entangled two-qubit states $|\phi\rangle$ [Bennett *et al.*,

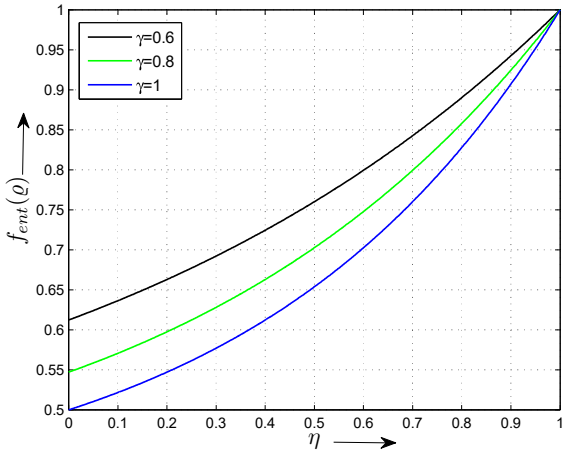

Figure 2.19 : Amount of fully-entangled fraction (FEF) as a function of weak measurement strength η at different values of decoherence parameter γ.

1996c; Horodecki *et al.*, 1999a]. Entanglement witnesses facilitate the experimental detection of entanglement and exist as a result of Hahn-Banach theorem [Horodecki, 1996; Terhal, 2000; Holmes, 2012]. Moreover, FEF is considered as an emerging tool in describing many practical quantum information processing protocols [Zhou and Guo, 2000; Vidal *et al.*, 2000; Albeverio *et al.*, 2002b; Grondalski *et al.*, 2002; Zhao *et al.*, 2003; Özdemir *et al.*, 2007; Li *et al.*, 2008; Zhao *et al.*, 2010; Li *et al.*, 2012; Kumar *et al.*, 2013]. For quantum teleportation, Horodecki *et al.* [Horodecki *et al.*, 1999a] have shown that a shared bipartite entangled state is useful for teleportation iff $f_{ent} > \frac{1}{2}$, where the relation between FEF and the optimal teleportation fidelity F_{max} is given by

$$F_{max} = \frac{2f_{ent} + 1}{3} \tag{2.53}$$

Since teleportation fidelity of the proposed class of states is always greater than $2/3$, FEF of the proposed class of states is always grater than $1/2$. Figure 2.19 indicates the same by showing the effect of weak measurement strength on FEF of the proposed state at three different values of amplitude-damping parameter.

We further consider three different witnesses to measure entanglement and correlations in the proposed class of states, namely, modified or rescaled version of FEF [Bartkiewicz *et al.*, 2017], nonlinear entropic measure [Bovino *et al.*, 2005] and Horodecki's measure $M(\rho)$ [Horodecki, 1996]. The modified FEF detects a larger set of entangled states in comparison to the other two measures. For this, Bartkiewicz *et al.* proposed an efficient and realistic experimental procedure based on entanglement swapping to detect entanglement using modified FEF, defined as

$$F^W = \frac{1}{2}\left(Tr\sqrt{U} - 1\right) = 2f_{ent} - 1 \tag{2.54}$$

where $F^W < 0$ corresponds to separable states, and maximum value of $F^W = 1$ correspond to maximally entangled states.

The form of nonlinear entropic entanglement witness [Bovino *et al.*, 2005] is given by

$$E^W = \frac{1}{2}\left(TrU + \left|Tr\rho_a^2 - Tr\rho_b^2\right| - 1\right) \tag{2.55}$$

where the value of E^W varies from 0 for separable states to 1 for maximally entangled two-qubit states. In addition, for quantifying nonlocal correlations in two-qubit states one may define Horodecki's measure $M(\rho)$ [Horodecki, 1996] as

$$M^W = TrU - \min\left[\text{eig}(U)\right] - 1 = M(\rho) - 1 \tag{2.56}$$

which is greater than 0 if a two-qubit state violates the Bell-CHSH inequality and attains the maximum value 1 for a maximally entangled state. $M(\rho)$ is directly related to the degree of Bell-CHSH inequality violation, such that $B'(\rho) = \sqrt{\max\left[0, M^W\right]}$ [Miranowicz, 2004; Horst *et al.*, 2013].

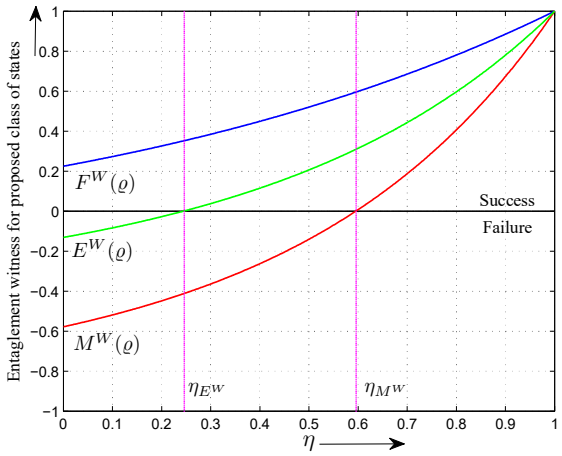

Figure 2.20 : Estimating the entanglement of proposed class of states using the Bell nonlocality measure M^W, nonlinear entanglement witness E^W and the rescaled FEF F^W as a function of weak measurement strength η, considering $\gamma = 0.6$.

Figure 2.20 shows that proposed class of states are always entangled for the complete range of weak measurement strength η for $\gamma = 0.6$, thereby highlighting the importance of the proposed class of states for quantum information processing protocols. However, linear entropic witness E^W and Bell nonlocality measure M^W can detect the entanglement and nonlocality in proposed class of states for $\eta_{E^W} \geq max\left\{0, (1 - \frac{0.4534}{\gamma})\right\}$, and $\eta_{M^W} \geq max\left\{0, (1 - \frac{0.2428}{\gamma})\right\}$, respectively.

Table 2.1 : Fully-entangled fraction (f_{ent}) and Nonlocality (B') measures of the proposed states ϱ^k (for k = 1, ..., 6) for different values of γ and η

State	γ	η	f_{ent}	B'
ϱ^1	0.6	0.4126	0.7288	0.0000
ϱ^2	0.6	0.4984	0.7596	0.3217
ϱ^3	0.8	0.7000	0.7994	0.4922
ϱ^4	0.4	0.6000	0.8581	0.6738
ϱ^5	0.1	0.6000	0.9611	0.9199
ϱ^6	0.6	0.9970	0.9982	0.9963

We further compare the fully-entangled fraction of the proposed class of states for a given degree of nonlocality $B'(\varrho)$ with randomly generated two-qubit states [Horst *et al.*, 2013]. For

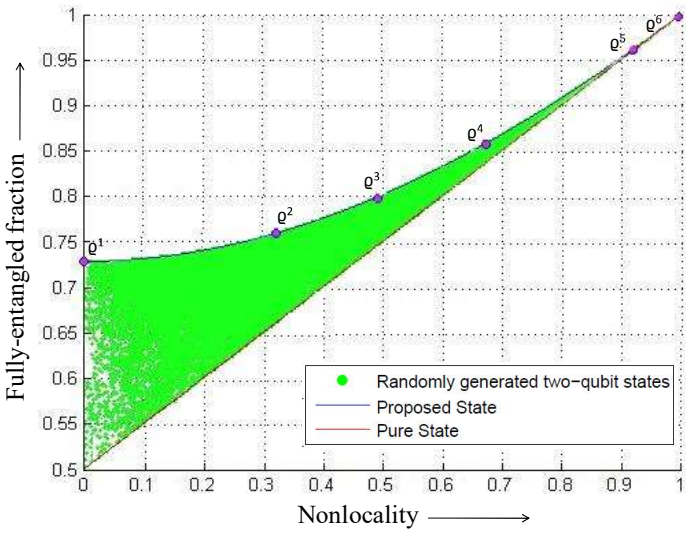

Figure 2.21 : Estimation of fully-entangled fraction for a given nonlocality for proposed class of states, pure states and randomly generated two-qubit states (green area) and the coordinates of points ϱ^k (where k=1,...6) to characterize the proposed class of states, given in Table 2.1.

example, Figure 2.21 numerically estimates the fully-entangled fraction of proposed class of states, pure states and 10^6 randomly generated two-qubit states. It shows that the proposed class of states have higher FEF than pure states and a large set of mixed two-qubit states for a given nonlocality. Here, we have only considered the states lying between our states and pure states. In Table 2.1, we present characteristic points ϱ^k (where k=1,...6) for different values of η and γ.

2.4.3 Dense coding

Superdense coding is one of the simplest application of quantum information processing [Bennett and Wiesner, 1992]. Usefulness of any shared entangled resource in dense coding is measured in terms of channel capacity, i.e., the maximum number of classical bits transmitted from a sender to a receiver using the shared resource [Bowen, 2001], where the channel capacity

using a bipartite entangled state ρ^{AB} shared between Alice and Bob is given by

$$C_{max} = \log_2 D_A + S(\rho^B) - S(\rho^{AB}) \tag{2.57}$$

where D_A is the dimension of Alice's subsystem, $S(\rho^B)$ is the von-Neumann entropy of Bob's subsystem ρ^B and $S(\rho^{AB})$ is the von-Neumann entropy of entangled state ρ^{AB}.

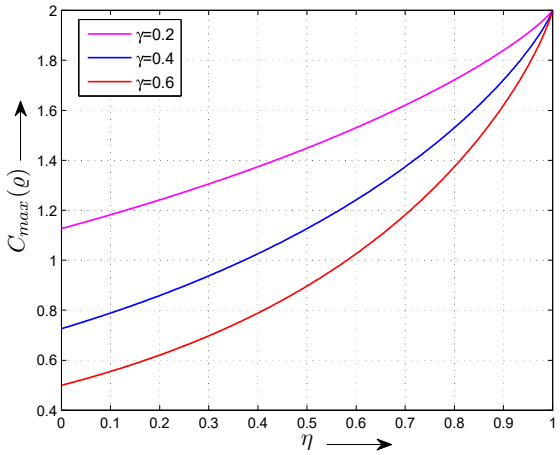

Figure 2.22 : Channel capacity of the proposed class of states ϱ for superdense coding protocol as a function of weak measurement strength η at three different values of decoherence parameter γ.

Figure 2.22 suggests that the channel capacity of the proposed class is always greater than 1 for weak decoherence, and increases with increase in the value of weak measurement strength. However, for strong decoherence, channel capacity only exceeds the classical channel capacity for large values of weak measurement strength. Therefore, our states are useful resources for superdense coding even at high decoherence for certain ranges of η. Furthermore, Figure 2.23 compares the efficiency of the proposed class with Werner states, Horodecki states, and ρ_{MEMS} for superdense coding in term of channel capacity. It clearly shows that our states are better resources for superdense coding in comparison to Werner states, Horodecki states, and ρ_{MEMS} states.

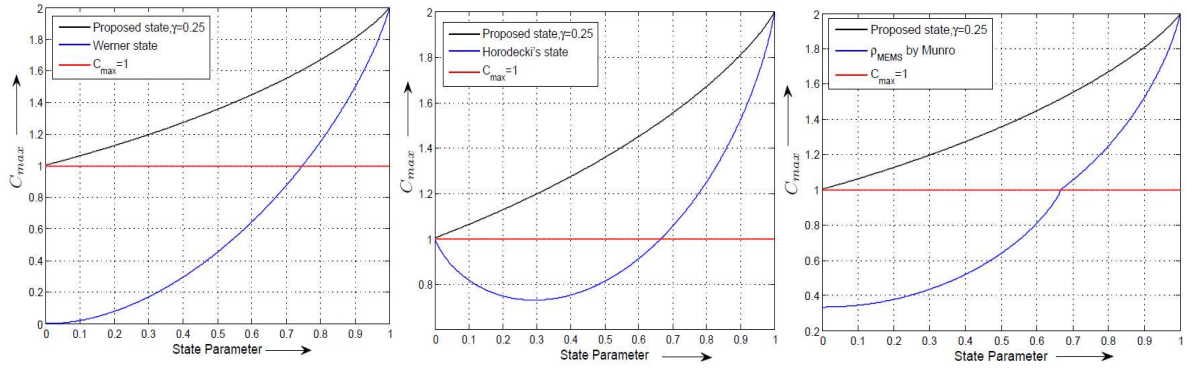

2.23 (a) : Comparison of the channel capacity of proposed class of states and Werner state.

2.23 (b) : Comparison of the channel capacity of proposed class of states and Horodecki state.

2.23 (c) : Comparison of the channel capacity of proposed class of states and MEMS state proposed by Munro *et. al.*

Figure 2.23 : Comparison of channel capacity of the proposed class with other bipartite entangled mixed states.

2.5 SUMMARY

In this chapter, we readdressed the issue of usefulness of two-qubit mixed states under noisy conditions. For this, we demonstrated an analytical relation between Bell-CHSH inequality with state parameter, noise parameters and weak measurement strength parameters. The analysis allowed us to propose a new class of two-qubit mixed entangled states for quantum information processing protocols. The study presented here proved to be useful as our class of states is shown to be better resources in comparison to many other two-qubit mixed states proposed earlier for the similar communication protocols.

…